

Electronic structures of an epitaxial graphene monolayer on SiC(0001) after gold intercalation:
a first-principles study

This article has been downloaded from IOPscience. Please scroll down to see the full text article.

2011 Nanotechnology 22 275704

(<http://iopscience.iop.org/0957-4484/22/27/275704>)

View [the table of contents for this issue](#), or go to the [journal homepage](#) for more

Download details:

IP Address: 163.28.112.100

The article was downloaded on 14/09/2011 at 02:58

Please note that [terms and conditions apply](#).

Electronic structures of an epitaxial graphene monolayer on SiC(0001) after gold intercalation: a first-principles study

Feng-Chuan Chuang^{1,4}, Wen-Huan Lin¹, Zhi-Quan Huang¹,
Chia-Hsiu Hsu¹, Chien-Cheng Kuo¹, Vidvuds Ozolins² and V Yeh³

¹ Department of Physics, National Sun Yat-Sen University, Kaohsiung 804, Taiwan

² Department of Materials Science and Engineering, University of California, Los Angeles, CA 90095-1595, USA

³ Department of Physics, National Dong Hwa University, Hualien 97401, Taiwan

E-mail: fchuang@mail.nsysu.edu.tw

Received 1 March 2011, in final form 19 April 2011

Published 20 May 2011

Online at stacks.iop.org/Nano/22/275704

Abstract

The atomic and electronic structures of an Au-intercalated graphene monolayer on the SiC(0001) surface were investigated using first-principles calculations. The unique Dirac cone of graphene near the K point reappeared as the monolayer was intercalated by Au atoms. Coherent interfaces were used to study the mismatch and the strain at the boundaries. Our calculations showed that the strain at the graphene/Au and Au/SiC(0001) interfaces also played a key role in the electronic structures. Furthermore, we found that at an Au coverage of 3/8 ML, Au intercalation leads to a strong n-type doping of graphene. At 9/8 ML, it exhibited a weak p-type doping, indicative that graphene was not fully decoupled from the substrate. The shift in the Dirac point resulting from the electronic doping was not only due to the different electronegativities but also due to the strain at the interfaces. Our calculated positions of the Dirac points are consistent with those observed in the ARPES experiment (Gierz *et al* 2010 *Phys. Rev. B* **81** 235408).

(Some figures in this article are in colour only in the electronic version)

1. Introduction

Graphene has attracted huge research interest due to its unique electronic properties and future applications. It is a gapless semiconductor with linear band dispersion near the K point, in which electrons behave as massless fermions. Recently, epitaxial graphene on SiC(0001) and SiC(000 $\bar{1}$) have been extensively studied due to the demand of large-scale production [1–9]. Unlike exfoliated graphene, the interaction between graphene and its supporting substrate usually plays a significant role in manipulating its electronic properties. A shift in the Fermi level above the Dirac point by 0.42 eV was found for graphene above the graphite layer on SiC(0001), which was ascribed to the n-type doping from the SiC(0001) substrate [1–5]. A substrate-induced energy gap was also

observed in epitaxial graphene on SiC(0001) owing to the sublattice symmetry breaking [1, 2]. In contrast, in order to create free-standing graphene, it is necessary to decouple it from the substrate via insertion of a buffer layer between graphene and the SiC(0001) substrate.

Based on the preceding idea, decoupling of graphene has previously been achieved by depositing molecules [7] or an atomic layer of Bi and Sb [6] while Guisinger *et al* have exposed the graphitized SiC to hydrogen in order to passivate dangling bonds at the interface [10]. Furthermore, Riedl *et al* have shown that the hydrogen intercalation can induce the desired decoupling [11]. An atomic model in which the hydrogens break the Si–C bonds at the interface and saturate the Si dangling bonds, leaving graphene to behave as a quasi-free-standing sheet was proposed. The atomic structures of the decoupled graphene were further studied by Lee *et al* [12] using first-principles calculations.

⁴ Author to whom any correspondence should be addressed.

Very recently, Gierz *et al* [13] demonstrated that the strongly interacting first graphitic layer was decoupled from the SiC(0001) substrate via gold intercalation. The atomic structures and effect of strain at the interfaces of graphene/Au and Au/SiC(0001) are still unclear. Thus, a first-principles study which is aimed at understanding the atomic and electronic structures, as well as the effect of strain at the interfaces, is highly desirable.

In this work, the atomic and electronic structures of the gold intercalation of graphene on SiC(0001) are studied in detail using first-principles calculations. We propose the atomic structures corresponding to the Au-intercalated graphene on SiC(0001). Furthermore, we incorporate the effect of strain and find that the calculated Dirac points are in excellent agreement with the measured ones. The rest of this paper is organized as follows: in section 2, we introduce our computational methods. Next, the atomic and electronic structures are analyzed and presented in section 3. Finally, we summarize our major findings with a brief conclusion in section 4.

2. Computational methods

The calculations were carried out within the generalized gradient approximation (GGA) to density functional theory [14, 15] using a projector-augmented-wave pseudopotential [16], as implemented in the *Vienna ab initio Simulation Package* [17]. The kinetic energy cutoff is set to 400 eV. The calculated lattice constants for crystalline 4H-SiC in the wurtzite structure are $a = 3.088$ and $b = 10.111$ Å, and that for bulk Au in face-centered cubic structure is 4.172 Å. The length of the 1×1 unit cell of graphene is 2.468 Å. Just as in the previous calculations [5, 4, 12], the $\sqrt{3} \times \sqrt{3}R30^\circ$ unit cell of SiC(0001) was used to match the 2×2 unit cell of graphene. As a result, the lengths of the supercells are 5.349, 5.110 and 4.936 Å for SiC(0001)- $\sqrt{3} \times \sqrt{3}$, Au(111)- $\sqrt{3} \times \sqrt{3}$ and 2×2 graphene, respectively. To take the mismatch into account, coherent interfaces were used. Note that two extreme considerations were used in previous studies [4, 5, 12]. One is that graphene is under about 8% tensile strain [4, 5] and the other is that the SiC(0001) surface experiences about 7% compressive strain [12].

The coverage of deposited Au is defined as the ratio of the number of Au atoms with respect to the number of C atoms in a 2×2 supercell of graphene. There are eight carbon atoms in the 2×2 supercell. However, the 2×2 supercell corresponds to three topmost Si atoms for SiC(0001) $\sqrt{3} \times \sqrt{3}$. Therefore, three and nine Au atoms within SiC(0001) $\sqrt{3} \times \sqrt{3}$ are, respectively, equal to 3/8 ML and 9/8 ML. These coverages roughly correspond to the experimental coverages of 1/3 and 1 ML [13]. Different thicknesses of 4H-SiC(0001) were used throughout our study. A vacuum layer of 12 Å is included in the supercell. The bottom carbon atoms were passivated by H atoms. Except for the bottom hydrogens and carbons, the rest of the atoms were relaxed until the residual force on each atom was smaller than 0.01 eV \AA^{-1} .

We noted that several Monkhorst–Pack grids [18] were used in previous studies [4, 5, 12]. Varchon *et al* [4] and

Mattausch *et al* [5] used the $9 \times 9 \times 1$ and $7 \times 7 \times 1$ grids, respectively, for studying graphene on SiC(0001). For the H-intercalated graphene, Lee *et al* used a $4 \times 4 \times 1$ grid [12]. Therefore, before embarking on any serious calculations, the convergence due to the density of the grid should be addressed. An equivalent $9 \times 9 \times 1$ Monkhorst–Pack grid sampling for 2×2 graphene in a previous study [4] may be sufficient to reach convergence in the atomic structures. However, it may not be accurate enough for band structure calculations for elements with a d orbital. The positions of the Dirac points versus the use of the k -point grid using the SiC(0001) $\sqrt{3} \times \sqrt{3}$ surface were tested and we found that a denser $21 \times 21 \times 1$ grid sampling should be used for the Brillouin zone integration. The density of the k -point grid is similar to that found in recent studies [19, 20]. Note that one of the grid points should lie right on the k -point in order to evaluate the Fermi level accurately for the p-type doping.

3. Results and discussion

After examining the accuracy due to the density of the k -point mesh, we turn to atomic structures of the Au-intercalated graphene/SiC(0001). First, we constructed the atomic structure in which the Au is intercalated between graphene and SiC(0001) at a coverage of 3/8 ML. Four bilayers of 4H-SiC(0001) are used to simulate the SiC(0001) substrate. We first set the periodicity of the supercell to that of SiC(0001) $\sqrt{3} \times \sqrt{3}$, which means graphene is under 8.4% tensile strain. Several structures were examined including those where some of the Au atoms are above graphene and we found that the lowest energy structure is one in which the Au is intercalated between graphene and the SiC(0001) substrate as shown in figure 1(b). We noticed that there are two relative positions of graphene above the Au layer, as shown in figures 1(c) and (f). The energy difference between them is rather small and there is no significant effect on the electronic structures. We will use the atomic structure of figure 1(c) for the rest of the study. It seems that the Au atoms break the Si–C bonds and that they bond with Si atoms, leaving graphene seemingly suspended above the Au layer. The vertical distance between graphene and the Au layer is around 3.03 Å. The lateral distance between Au and Au atoms is 3.09 Å, which is close to 2.95 Å, the length of the Au(111) 1×1 . We can regard the Au layer as the Au(111) surface expanded by 4.7%.

Unlike previous calculations [5, 4, 12], we believe that the mismatches at the graphene/Au and Au/SiC(0001) interfaces should be considered. Therefore, lateral strains were applied to the coherent interface and their atomic structures were also relaxed. This method has been used to study the strain in different surface systems [21–24]. The relative energies versus the strain of graphene are plotted in figure 2(a). The lowest energy is set to zero and the strain is defined with respect to the periodicity of graphene. The strain with the lowest energy is about 5.9%. However, the band structure for strain at 8.4% is shown in figure 2(b). We used similar definitions for the Dirac point and induced gap as those employed in the study by Zhou *et al* [3]. In figure 2(c), the calculated Dirac point is -0.83 eV (e.g. 0.83 eV below the Fermi level) which is consistent with

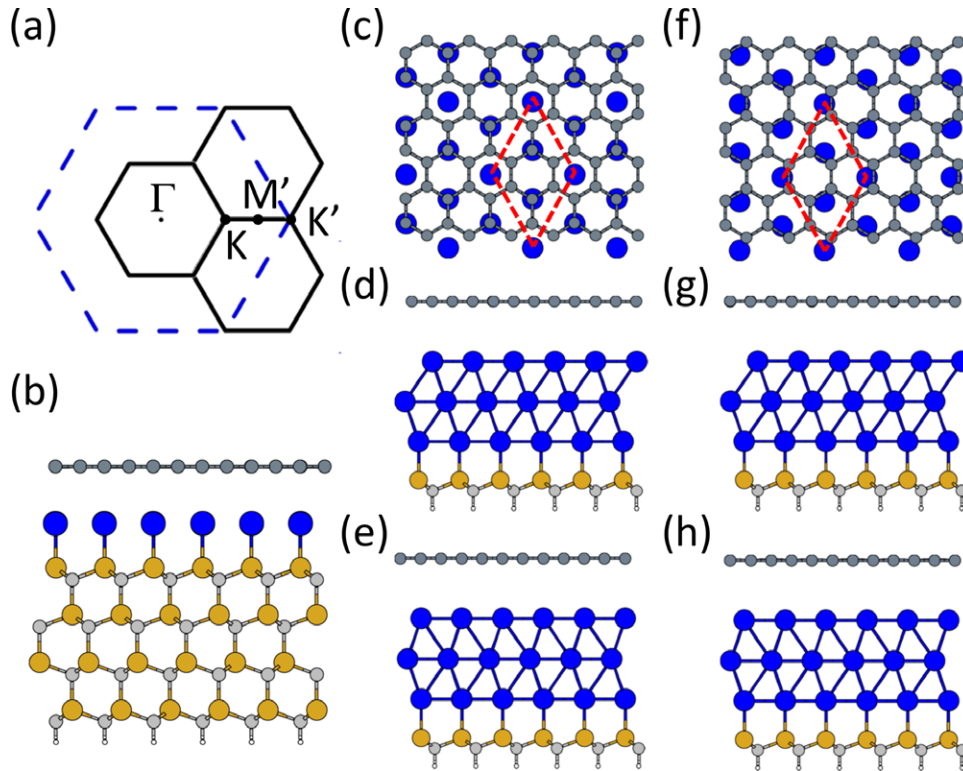


Figure 1. (a) The dashed lines and solid lines indicate the Brillouin zones of the 1×1 unit cell and 2×2 supercell of graphene, respectively. Specific k -points are labeled. (b) shows the side view of the atomic model for Au-intercalated graphene on SiC(0001) at a coverage of $3/8$ ML. (c) and (f) show the top views of graphene and topmost Au layer. The corresponding side views of the atomic structures of Au-intercalated graphene on SiC(0001) at $9/8$ ML for Au layers in FCC and HCP, respectively, corresponding to the top view in (c) are shown in (d) and (e). (g) and (h) show the side views of the atomic structures of Au-intercalated graphene on SiC(0001) at $9/8$ ML for Au layers in FCC and HCP, respectively, corresponding to top view (f).

the experimental value of -0.85 eV. The induced gap is quite small and found to be 0.03 eV. To understand how the Dirac point changes as the strain is varied, we calculated the band structures and located the Dirac points for four special cases. The first case is graphene without strain, while the second is graphene under 3.5% strain and the third is the strain with the lowest energy. The fourth is the SiC(0001) without strain. The respective positions of the Dirac points are -0.23 , -0.33 , -0.67 and -0.83 eV, as shown in figure 2(a). Though at 5.9% strain, the system has the lowest energy we found that at 8.4% strain the Dirac point is in excellent agreement with experimental observations [13].

Next, we constructed the atomic structure of Au intercalation between graphene and SiC(0001) at an Au coverage of $9/8$ ML. Two possible stackings of Au between graphene and SiC(0001) were proposed. One is the ABC stacking (face-centered cubic), while the other is the ABA stacking (hexagonal close-packed) as shown in figures 1(d) and (e). The corresponding top view is shown in figure 1(c), similar to as in $3/8$ ML. Figures 1(g) and (h) are side views corresponding to the top view 1(f). The same approaches were used to locate the strain with the lowest energy. Two bilayers of SiC(0001) is included in the coherent interface rather than four bilayers. We also noted that the energy difference between atomic structures of figures 1(c) and (f) at an Au coverage of $9/8$ ML is rather small and there is no significant effect

in the electronic structures. The variations of energy versus strain of graphene are shown in figure 3(a). Only the curves corresponding to the top atomic structures of figure 1(c) are shown. The energy curve of ABC stacking (FCC) of Au(111) is slightly lower than that of the ABA stacking (HCP) in figure 3(a). The strains with the lowest energy for both stackings are found to be 3.9% . The corresponding band structures for FCC are shown in figures 3(b) and (c). The calculated Dirac points are $+0.11$ and $+0.09$ eV for FCC and HCP, respectively, while the experimental value is at $+0.10$ eV. Similarly, four special cases were also examined in figure 3(a) which show that the corresponding positions of the Dirac points are $+0.38$ ($+0.38$), $+0.10$ ($+0.13$), $+0.11$ ($+0.09$) and -0.03 (-0.04) eV for FCC (HCP). We also found that, when graphene is under 2.6% strain, the Dirac point matches the experimental value well.

To understand the effect of the SiC(0001) substrate on graphene/Au(111) and the lattice mismatch between two interfaces (graphene/Au and Au/SiC(0001)) at $9/8$ ML, we also plotted the energy versus strain without the supporting SiC(0001) substrate. The lowest energy condition is when graphene is at 0% strain, i.e. Au layers are compressed by 3.4% . Owing to the high ductility and malleability of Au, it is plausible that Au layers are compressed to match the periodicity of graphene. However, the corresponding Dirac points for FCC and HCP are $+0.38$ and $+0.40$ eV, which differ

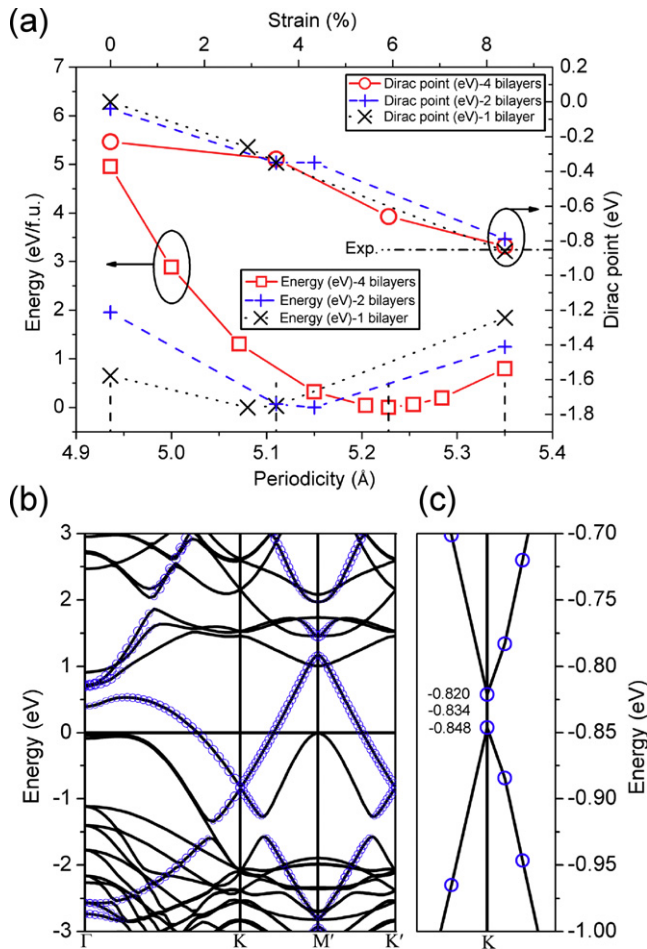


Figure 2. (a) The energies and Dirac points versus strain for Au-intercalated graphene on SiC(0001) at Au coverage of 3/8 ML. The lines serve as guides to the eye. (b) The band structure corresponds to strain at 8.4%. (c) The band structure near the k -point is magnified to determine the Dirac point and the induced gap.

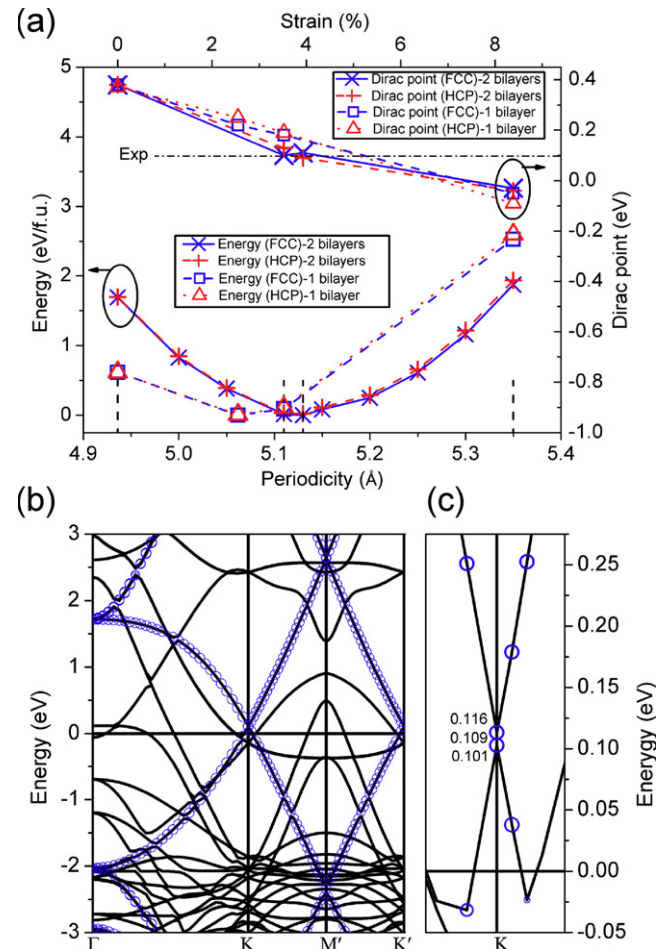


Figure 3. (a) The total energies and Dirac points versus strain for Au-intercalated graphene on SiC(0001) at coverage of 9/8 ML. The lines serve as guides to the eye. (b) The corresponding band structure of ABC stacking at 3.9% strain. (c) The band structure near the k -point is magnified to determine the Dirac point and the induced gap.

widely from the experimental value of 0.1 eV. The SiC(0001) substrate has a strong influence on the electronic doping. This also validated the periodicity setting used in recent studies in which metal substrates are compressed to match the length of graphene [19, 20]. They showed that the Dirac point for graphene chemisorbed on Au(111) is +0.19 eV. Note that six layers of Au(111) were used in [19, 20], while only three layers of Au(111) were employed in the present study.

Another issue worth exploring is the impact of the thickness of 4H-SiC(0001). Thus, in this study we varied the thickness of 4H-SiC(0001). The results are summarized in table 1 and figures 2(a) and 3(a). For a four-bilayer substrate, our calculations showed that at an Au coverage of 9/8 ML the strain with the lowest energy is 5.3%, whereas at an Au coverage of 3/8 ML it is 5.9%. For the same thickness of substrates, the periodicity of the interface with three Au layers is generally closer to that of Au(111) (around 3.5%) than that with one Au layer. Nonetheless, in terms of the position of Dirac point, for Au at 3/8 ML the best match to the experiment is graphene under 8.4% strain (e.g. SiC(0001) lattice constant), while for Au at 9/8 ML, the best match to the experiment is

graphene at around 3.5% strain (Au(111) lattice constant) as shown in figures 2(a) and (c).

In addition, the recalculated Dirac point for the two-carbon layer model (e.g. one graphene layer and one graphite buffer layer) [4] using a one-bilayer SiC(0001) substrate is -0.37 eV (see table 1) which is close to the experimental value of -0.42 eV. Note that the Dirac points were found to be -0.67 eV and -0.42 eV in studies by Varchon *et al* [4] (using a $9 \times 9 \times 1$ grid) and by Mattausch *et al* [5] (using a $7 \times 7 \times 1$ grid), respectively. In addition, our recalculated induced gap is close to zero which is similar to what they found in previous studies [4, 5], whereas the experimental value of the induced gap is about 0.26 eV [3].

Moreover, we constructed the atomic structure of H-intercalated graphene on SiC(0001) at an H coverage of 3/8 ML. Several structures were examined and we found that the lowest energy structure is one in which the H atoms saturate the topmost Si bonds of SiC(0001) resulting in a freestanding graphene. Our lowest energy structure is the same as that reported in a recent study by Lee *et al* [12]. The Dirac point in

Table 1. Strains, ε , with the lowest energies for different substrates, the corresponding Dirac points, E_D (eV), induced gaps, Δ (eV) and the Dirac points of graphene without the substrate under the same strain are listed. Graphene is labeled as G.

	θ (ML)	SiC(0001)		E_D	E_D exp.	E_D G	Δ (eV)	Δ exp.
		bilayers	ε (%)					
G/Au	3/8	1	2.9	-0.26		0.00	0.06	
G/Au	3/8	2	4.3	-0.35		0.00	0.00	
G/Au	3/8	4	5.9	-0.67	-0.85 ^a	0.00	0.04	
G/Au(FCC)	9/8	0	0.0	+0.38		0.00	0.00	
G/Au(HCP)	9/8	0	0.0	+0.40		0.00	0.00	
G/Au(FCC)	9/8	1	2.6	+0.22	+0.10 ^a	0.00	0.00	
G/Au(HCP)	9/8	1	2.6	+0.25	+0.10 ^a	0.00	0.00	
G/Au(FCC)	9/8	2	3.9	+0.11		+0.01	0.01	
G/Au(HCP)	9/8	2	3.9	+0.09		+0.01	0.01	
G/Au(FCC)	9/8	4	5.3	+0.01		0.00	0.02	
G/Au(HCP)	9/8	4	5.3	+0.03		0.00	0.00	
G/graphite	1	1	2.1	-0.37	-0.42 ^b	0.00	0.00	0.26 ^c
G/graphite	1	2	3.3	-0.39		0.00	0.00	
G/graphite	1	4	4.8	-0.40		-0.01	0.00	
G/H	3/8	1	3.1	0.01	+0.10 ^b	0.00	0.02	
G/H	3/8	2	4.5	-0.01		+0.01	0.02	
G/H	3/8	4	5.9	0.01		-0.01	0.03	

^a Reference [13]. ^b Reference [11]. ^c Reference [3].

that study [12] ($4 \times 4 \times 1$) is at -0.07 eV, while experimentally it is at $+0.10$ eV [11]. Furthermore, the energy versus strain plots were generated and it was found that the strain with the lowest energy was 3.1% for a one-bilayer SiC(0001) substrate as listed in table 1. The corresponding Dirac point is at 0.01 eV, barely above the Fermi level. The calculated Dirac points of both the current and previous studies [12] are both near the Fermi level. Our calculations indicate that H intercalation results in an almost fully decoupled graphene, though that Dirac point is off by $+0.09$ eV compared to that reported in the ARPES experiment [13]. Furthermore, the induced gap is found to be 0.02 eV.

By using the position of the Dirac point as an indicator, we can estimate the depth of the interface regime. It is clear that the mismatch at the interfaces seems to propagate into the uppermost layers of the SiC(0001) substrate while the lower still retains its ideal lattice constant. The bond strengths will apparently affect the depth of the interface regime. In the case of the two-carbon layer model [4], as well as the intercalation models with an H coverage of 3/8 ML [12] the coherent interface includes only the topmost SiC(0001) bilayer. For the model with an Au coverage of 9/8 ML (forming three Au layers), the top Au and bottom Au layers have strong bonding with graphene and SiC(0001), respectively. However, the intermediate Au layer has high ductility and malleability and thus behaves as a cushion. As a result, two SiC(0001) bilayers are considered to be included in the interface regime.

The reader might suspect that the shift of the Dirac point probably results from the effect of strain. To confirm this, the Dirac points of the single sheet of graphene under the aforementioned strains were also calculated. Our results were summarized in table 1. They clearly show that the change in the Dirac point due to strain is less than 0.02 eV and can be ignored.

We noted that the force convergence criterion for atomic relaxation after applied strain affects the distance between graphene and substrate. This would also result in

different amount of charge transfer between graphene and substrate [19, 20], thus change the position of the Dirac point.

Finally, we also calculated the induced gaps, Δ , for all our calculations. As table 1 shows, the calculated induced gaps are all close to zero and inconsistent with the experimental value of 0.26 eV for the two-carbon layer model (e.g. graphene and one graphite buffer layer) on SiC(0001) [3]. We further examined the projected density of states for the cases listed in table 1 and found no obvious suppression of the density of state (DOS) around the center of the Dirac cone. We conclude that neither the strained interface nor suppressed DOS near the center of the Dirac cone causes the gap opening.

4. Conclusions

The atomic and electronic structures of an Au-intercalated graphene monolayer on an SiC(0001) surface are investigated using first-principles calculations. The unique Dirac cone of graphene near the K point reappear as the monolayer is intercalated by Au atoms. We have demonstrated an approach to study the mismatch and strain at the interfaces. Our calculations show that the strain at the graphene/Au and Au/SiC(0001) interfaces play a key role in the electronic structures. The shift of the Dirac point resulting from the electronic doping is not only due to the different electronegativities but also the strain at the interfaces. Our calculated positions of Dirac points are consistent with those observed in the ARPES experiment.

Acknowledgments

FCC acknowledges support from the National Center for Theoretical Sciences (NCTS) and the Taiwan National Science Council (NSC) under grant no. NSC-98-2112-M110-002-MY3. We are grateful to the National Center for High-Performance Computing (NCHC) for computer time and

facilities. VO was supported as part of the Molecularly Engineered Energy Materials (MEEM), an Energy Frontier Research Center funded by the US Department of Energy, Office of Science, Office of Basic Energy Sciences under Award Number DE-SC0001342.

References

- [1] Ohta T, Bostwick A, Seyller T, Horn K and Rotenberg E 2006 *Science* **313** 951
- [2] Bostwick A, Ohta T, Seyller T, Horn K and Rotenberg E 2007 *Nature Phys.* **3** 36
- [3] Zhou S Y, Gweon G-H, Fedorov A V, First P N, de Heer W A, Lee D-H, Guinea F, Castro Neto A H and Lanzara A 2007 *Nat. Mater.* **6** 770
- [4] Varchon F *et al* 2007 *Phys. Rev. Lett.* **99** 126805
- [5] Mattausch A and Pankratov O 2007 *Phys. Rev. Lett.* **99** 076802
- [6] Gierz I, Riedl C, Starke U, Ast C R and Kern K 2008 *Nano Lett.* **8** 4603
- [7] Coletti C, Riedl C, Lee D S, Krauss B, Patthey L, von Klitzing K, Smet J H and Starke U 2010 *Phys. Rev. B* **81** 235401
- [8] Park C-H, Giustino F, Spataru C D, Cohen M L and Louie S G 2009 *Nano Lett.* **9** 4234
- [9] Kim S, Ihm J, Choi H J and Son Y-W 2008 *Phys. Rev. Lett.* **100** 176802
- [10] Guisinger N P, Rutter G M, Crain J N, First P N and Stroscio J A 2009 *Nano Lett.* **9** 1462
- [11] Riedl C, Coletti C, Iwasaki T, Zakharov A A and Starke U 2009 *Phys. Rev. Lett.* **103** 246804
- [12] Lee B, Han S and Kim Y-S 2010 *Phys. Rev. B* **81** 075432
- [13] Gierz I *et al* 2010 *Phys. Rev. B* **81** 235408
- [14] Hohenberg P and Kohn W 1964 *Phys. Rev.* **136** B864
Kohn W and Sham L J 1965 *Phys. Rev.* **140** A1135
- [15] Perdew J P, Burke K and Ernzerhof M 1996 *Phys. Rev. Lett.* **77** 3865
- [16] Kresse G and Joubert D 1999 *Phys. Rev. B* **59** 1758
- [17] Kresse G and Hafner J 1993 *Phys. Rev. B* **47** 558
Kresse G and Furthmuller J 1996 *Phys. Rev. B* **54** 11169
- [18] Monkhorst H J and Pack J D 1976 *Phys. Rev. B* **13** 5188
- [19] Giovannetti G, Khomyakov P A, Brocks G, Karpan V M, van den Brink J and Kelly P J 2008 *Phys. Rev. Lett.* **101** 026803
- [20] Khomyakov P A, Giovannetti G, Rusu I P C, Brocks G, van den Brink J and Kelly P J 2009 *Phys. Rev. B* **79** 195425
- [21] Lu G-H, Cuma M and Liu F 2005 *Phys. Rev. B* **72** 125415
- [22] Chuang F C 2007 *Phys. Rev. B* **75** 115408
- [23] Su W S, Chuang F C, Lin K M and Leung T C 2010 *J. Vac. Sci. Technol. A* **28** 1366
- [24] Ciobanua C V and Briggs R M 2006 *Appl. Phys. Lett.* **88** 133125